Framework Development for Numerical Modeling of the Low Wind Effect at Subaru Telescope

M. Koren, S. Vievard, B. Allen
University of Hawaiʻi at Mānoa, College of Engineering, SSEI
mkoren@hawaii.edu

NAOJ Mitaka, October 30th, 2025

Project Aim

- The **Low Wind Effect (LWE)** occurs when weak wind fails to mix air around telescope structures, creating temperature-driven refractive index variations that distort wavefronts.
- During SCExAO operations, LWE compromises over 30% of observing time, leading loss in operational time and money.
- Mitigation of LWE will become increasingly important with the wider adoption of Adaptive Optics (AO) and the arrival of Extremely Large Telescopes (ELTs).
- **Aim: Build a simulation environment to study LWE and test mitigation strategies.**
- This talk presents a preliminary **Computational Fluid Dynamics (CFD) model**, the core of the LWE simulation framework.

Simulation Inputs:

- Meteorological conditions
- Telescope position

Simulation Outputs:

- Optical Path Difference fields
- Point Spread Function (with optical simulation)

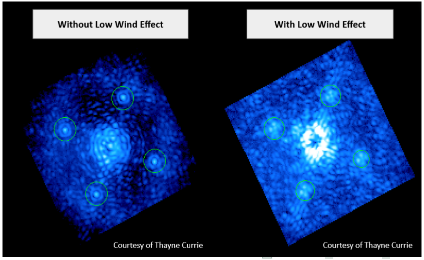

Table of Contents

Table of Contents

The **Low Wind Effect (LWE)** occurs when the telescope's secondary mirror support (*spider*) cools by radiating heat to the night sky, while weak ventilation fails to remove the resulting temperature gradients.

Physical phenomena:

- Spider radiates heat to the night sky
- Convection transfers heat from the surrounding air to the spider
- Temperature differences in the air modify the refractive index
- Non-uniform refractive index introduces **Optical Path Differences (OPD)**
- OPD causes wavefront distortions and image degradation

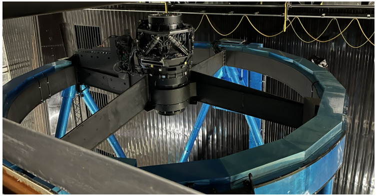

Spyder of the Subaru Telescope

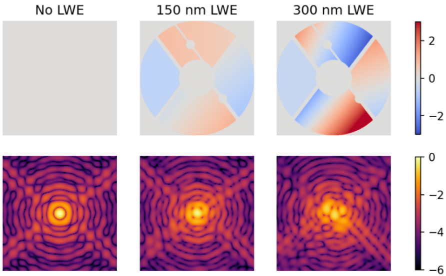

Simulation of the Low Wind Effect (Leboulleux et al., 2024)

Heat Transfers

1. Radiation The spider loses heat via thermal radiation to the night sky, modeled as a gray body:

$$\dot{Q}_{\mathrm{rad}} = \frac{\sigma\left(T_{\mathrm{sky}}^4 - T_{\mathrm{spider}}^4\right)}{\frac{1-\epsilon_{\mathrm{spider}}}{A_{\mathrm{spider}}\epsilon_{\mathrm{spider}}} + \frac{1}{A_{\mathrm{spider}}F_{\mathrm{spider}\to\mathrm{sky}}} + \frac{1-\epsilon_{\mathrm{sky}}}{A_{\mathrm{sky}}\epsilon_{\mathrm{sky}}}}$$

2. Convection Heat is transferred back from the surrounding air by convection:

$$\dot{Q}_{\mathrm{conv}} = hA_{\mathrm{spider}}(T_\infty - T_{\mathrm{spider}})$$

Heat transfer coefficient h depends on wind speed via the Nusselt number:

$$\mathrm{Nu}_f = \frac{hd}{k_f} = C\left(\frac{u_\infty d}{\nu_f}\right)^n \mathrm{Pr}_f^{1/3}$$

3. Equilibrium

$$\dot{Q}_{\mathrm{conv}} + \dot{Q}_{\mathrm{rad}} = 0 \qquad \Rightarrow \qquad (T_{\mathrm{spider}} - T_\infty) \sim u_\infty^{-n}$$

Example ($n = 0.588$):

$u_\infty = 3$ m/s $\Rightarrow (T_{\mathrm{spider}} - T_\infty) = -2$ K

$u_\infty = 1$ m/s $\Rightarrow (T_{\mathrm{spider}} - T_\infty) = -3.84$ K

Geometry	Re_{df}	C	n
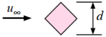	$5 \times 10^3 - 10^5$	0.246	0.588
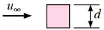	$5 \times 10^3 - 10^5$	0.102	0.675

Heat transfer constants for square-based cylinders (Holman, 2010)

The **Optical Path Length (OPL)** is obtained by integrating the refractive index along the light path:

$$OPL = \int_C n \, \mathrm{d}s$$

- **Refractive index:** Approximated by a simplified Ciddor equation (depends on T, p, and λ):

$$n = 1 + 7.76 \times 10^{-7} \, p_{ref} \, \frac{1 + 0.00752/\lambda^2}{T}$$

- **Optical Path Difference (OPD):** Calculated by integrating the refractive index difference along the path:

$$OPD = \int_C \Delta n \, \mathrm{d}s$$

Table of Contents

Computational Fluid Dynamics (CFD) models in OpenFOAM
Multiple scale → Multiple models

Model hierarchy (OpenFOAM):

- **Summit model**: Maunakea summit topography → boundary conditions
  Resolution: 10 m – 80 m
- **Main model**: Telescope, dome, surroundings
  Resolution: 0.08 m – 2.5 m
- **Vent model**: Vent covers → parameters for implicit cover model
  Resolution: 0.01 m

Physical assumptions:

- Steady-state simulation
- Incompressible fluid (Boussinesq approximation)
- Temperature field included
- Neutral stratification
- No radiation model
- k-ω SST turbulence model (RANS)

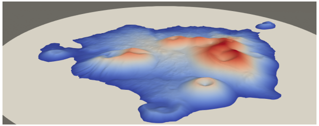

Summit model

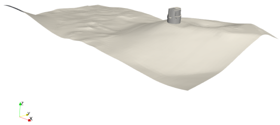

Main model

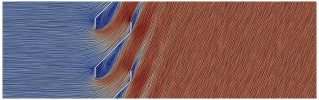

Vent model

Model Descriptions: Geometry sources

- Maunakea topography from USGS: horizontal resolution $9.26 \cdot 10^{-5\circ}$ ($\sim$10 m)
- Dome geometry from scanned blueprints (NAOJ), main features verified with measurements
- Telescope geometry: open-source 3D printable model (NAOJ)
- Shortcomings:
  - Dome geometry inaccuracies
  - Missing neighboring telescopes

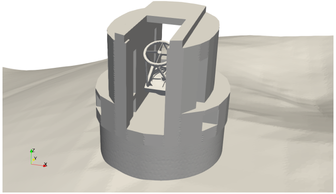

Dome geometry

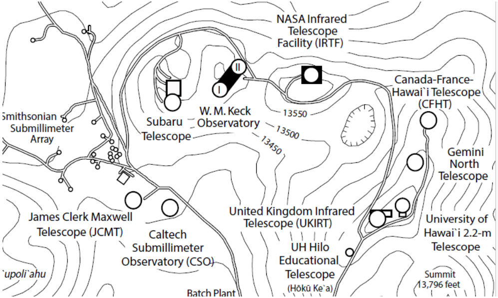

Map of the Maunakea

Summit model

- Maunakea summit (alt. > 3950 m)
- Circular summit area ($\sim$4.5 km diameter)
- Computational domain: 15 km $\times$ 15 km $\times$ 1 km
- Rotatable outer boundary

Main model

- Dome and telescope surroundings
- Oriented along flow direction
- Telescope orientation: south, elevation 60°
- Domain size: 440 m $\times$ 840 m $\times$ 142 m

Vent model

- Contains two cover elements
- Periodic model
- $2L \times 18L$

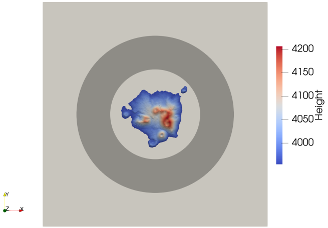

Summit model

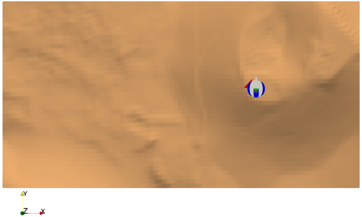

Main model

Vent model

Model Descriptions: Mesh

Summit model

- Cut-cell method with 4 resolutions (10–80 m)
- Boundary layer mesh:
  - First layer: 0.3 m
  - 12 layers, growth rate 1.2

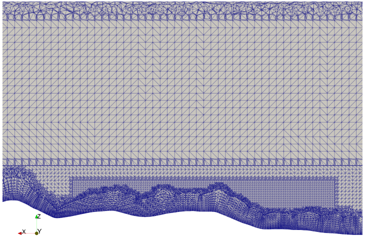

Summit model mesh

Main model

- Cut-cell method
- Base resolution: 2.5 m
- Refinements:
  - Dome far field: 1.25 m
  - Dome near field: 0.625 m
  - Telescope: 0.313 m
  - Top ring: 0.156 m
  - Spider: 0.078 m

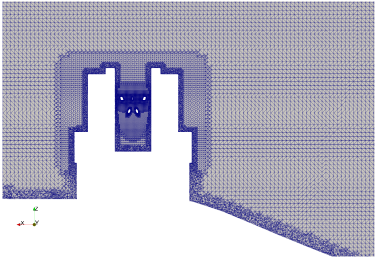

Main model mesh

Vent model

- 2D simulation
- Cubic elements
- Resolution: 0.01 m

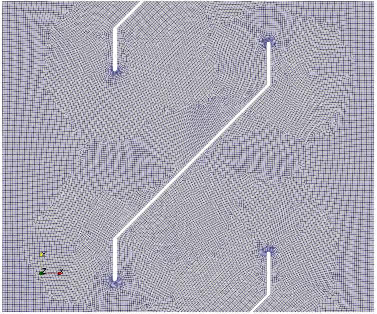

Vent model mesh

Large Model: Boundary Conditions

Summit model

- **Velocity inlet:** homogeneous, (East 1 m/s)
- **Pressure outlet:** 0 Pa
- **Summit:** atmospheric wall
- **Ground:** slip wall
- **Top & sides:** symmetry

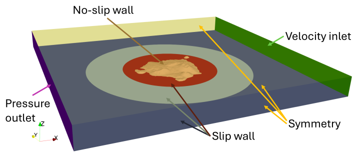

Summit model boundaries

Main model

- **Velocity inlet:** mapped
- **Outlet:** pressure 0 Pa
- **Summit:** atmospheric wall
- **Walls:** no-slip
- **Top & sides:** symmetry
- **Spider & ring:** $T_{ref} - \Delta T$
- **Vents:** volumetric force terms

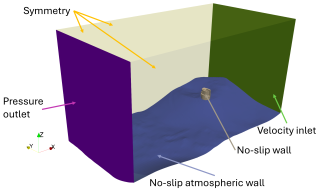

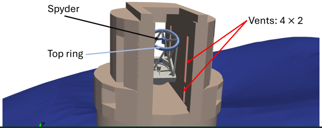

Vent model

- **Velocity inlet:** homogeneous, variable
- **Pressure outlet:** 0 Pa
- **Walls:** no-slip
- **Sides:** periodic
- **Top & bottom:** empty

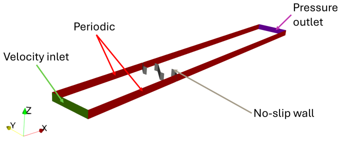

Vent model boundaries

Table of Contents

Vent cover the inner side of the ventilation channels. Each cover consists of 11 fixed metal sheets. Explicit CFD modeling would require too many mesh elements → replaced by **volume source terms**.
A periodic model was used to estimate pressure drop and velocity deflection at 5 inlet velocities.
Implicit source terms:

- **Darcy–Forchheimer source term:** models static pressure drop along vent direction

$$\nabla p = \mu \mathbf{D}\mathbf{U} + \frac{1}{2}\rho \,\mathrm{tr}(\mathbf{U}\cdot\mathbf{I})\,\mathbf{F}\mathbf{U}$$

  with $\mathbf{F}, \mathbf{D}$ fitted from pressure–velocity curves.

- **Pressure source term:** introduces a perpendicular pressure gradient to deflect flow

$$\nabla p = -C(\mathbf{U}\mathbf{e}_1)^2 \mathbf{e}_1\,(\mathbf{U}\mathbf{e}_1)/\|\mathbf{U}\mathbf{e}_1\|$$

  where C is derived from Navier–Stokes and $\mathbf{e}_1$ is the deflection direction.

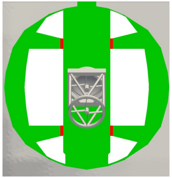

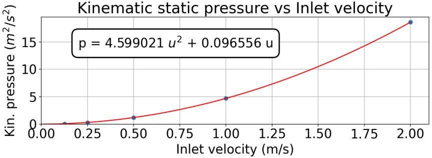

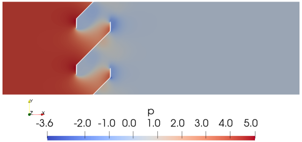

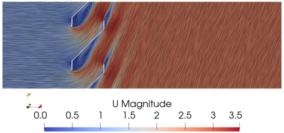

Kinematic pressure distribution and velocity magnitude around the cover at 1 m/s

Vent Model - Results

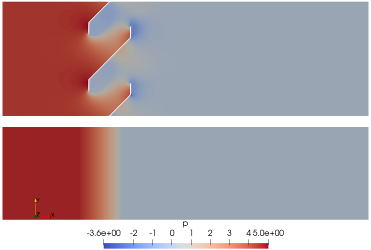

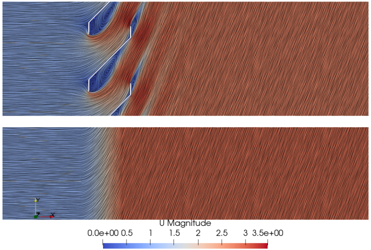

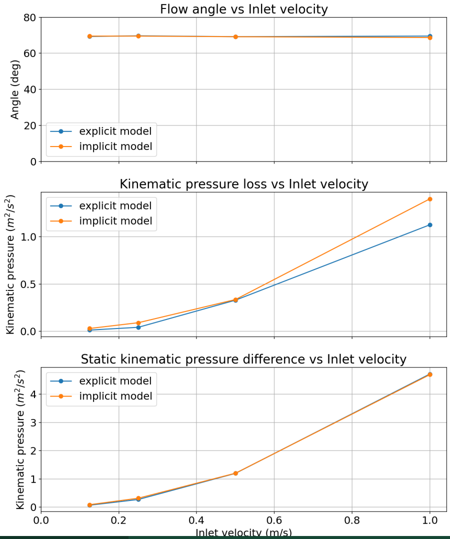

Large model: Results

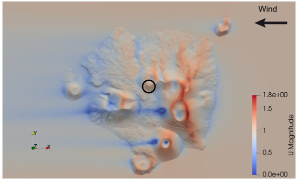

Velocity at 10 m above ground

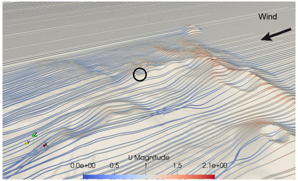

Streamlines colored by velocity magnitude

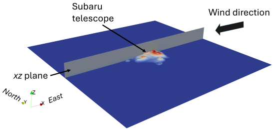

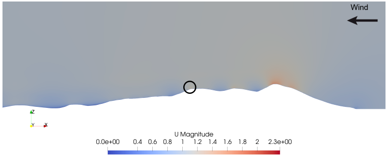

velocity

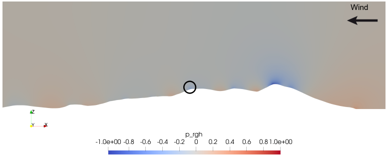

pressure

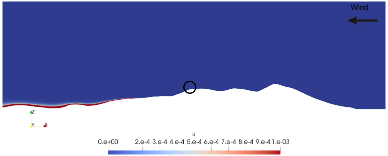

turbulent kinetic energy

Main model: Results - Global

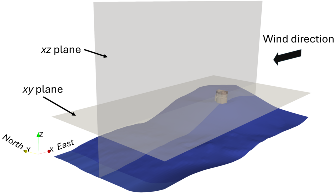

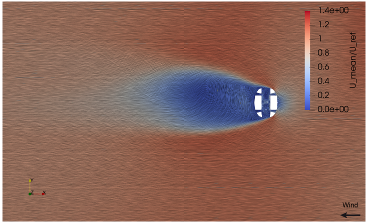

Dimensionless velocity magnitude, U / U_{ref}

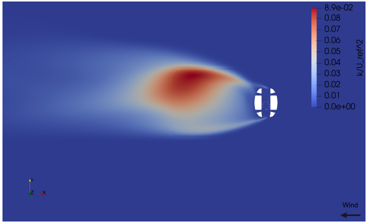

Dimensionless turbulent kinematic energy, k / U_{ref}^2

xy plane

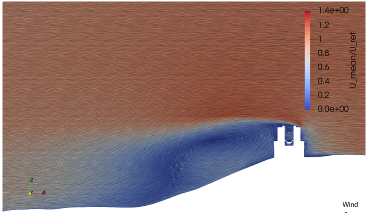

Dimensionless velocity magnitude, U / U_{ref}

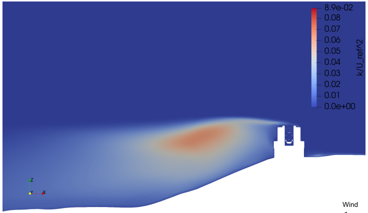

Dimensionless turbulent kinematic energy, k / U_{ref}^2

xz plane

Main model: Results - Dome

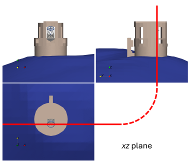

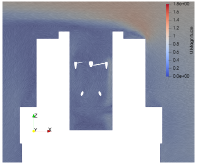

velocity

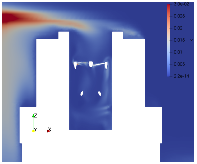

turbulent kinetic energy

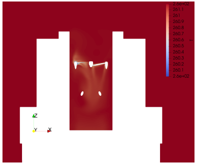

temperature

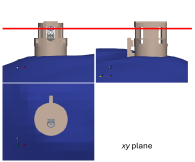

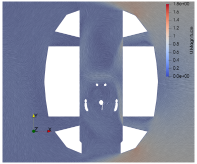

velocity

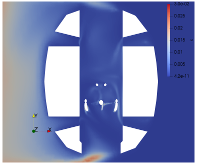

turbulent kinetic energy

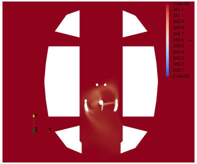

temperature

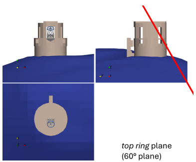

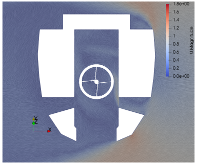

velocity

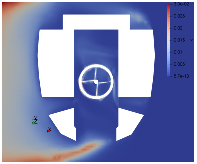

turbulent kinetic energy

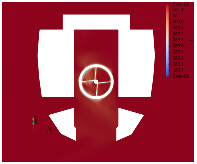

temperature

Main model: Result – 3D

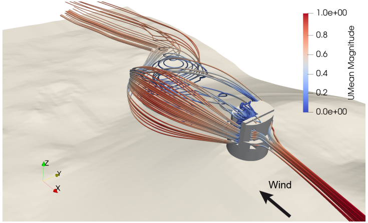

Streamlines windward side

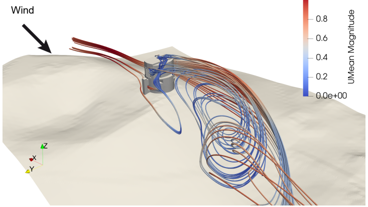

Streamlines leeward side

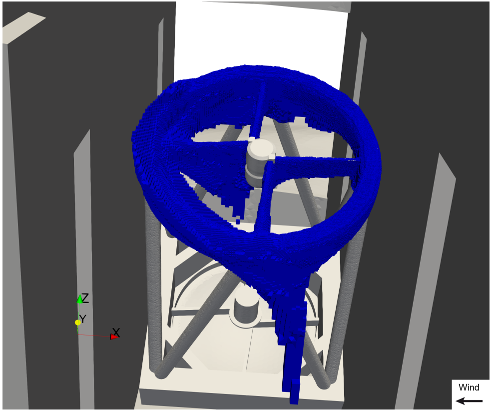

T_{ref} – 0.2 K air bubble

Main model: OPD and focal plane image

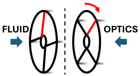

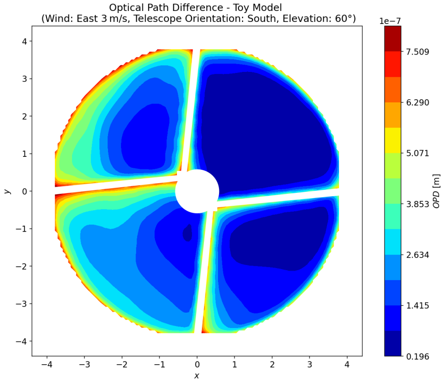

Optical Path Diffrence at the primary mirror

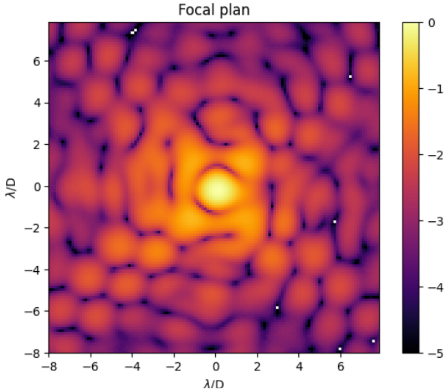

Point Spread Function at the focal plane;
Created by: Sebastien Vievard

Table of Contents

Different spider temperature: OPD

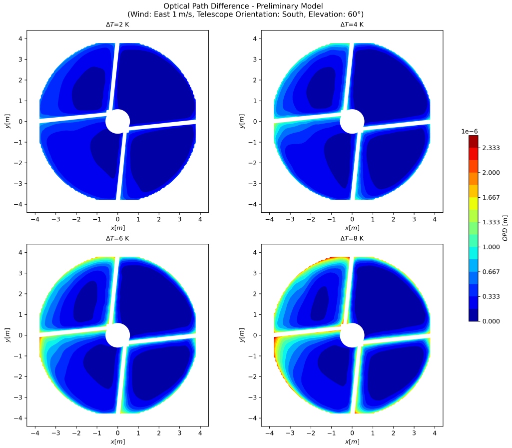

Optical Path Difference as a function of the spider temperature

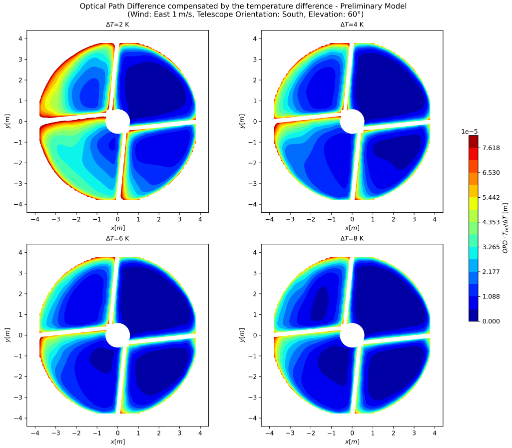

Optical Path Difference compensated by the temperature difference as a function of the spider temperature

$n^* = n \cdot T_{ref} / \Delta T$

Different spider temperature: OPD and focal plane image

2K

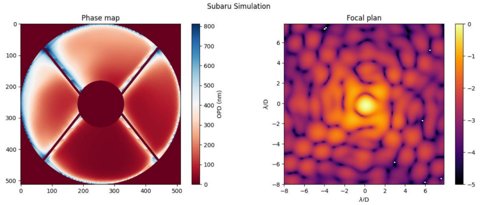

4K

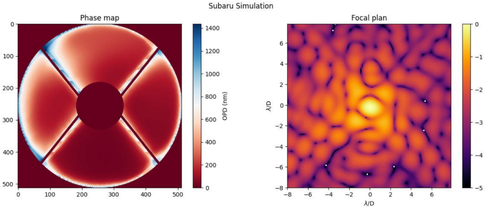

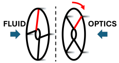

6K

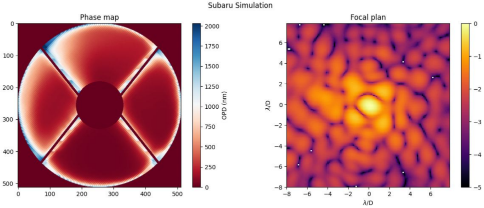

8K

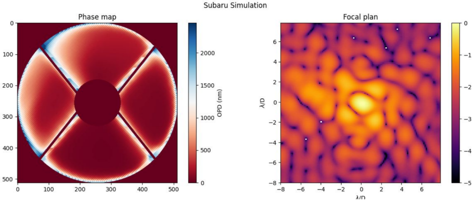

Different spider temperature: Contrast curves from simulated coronagraphic images

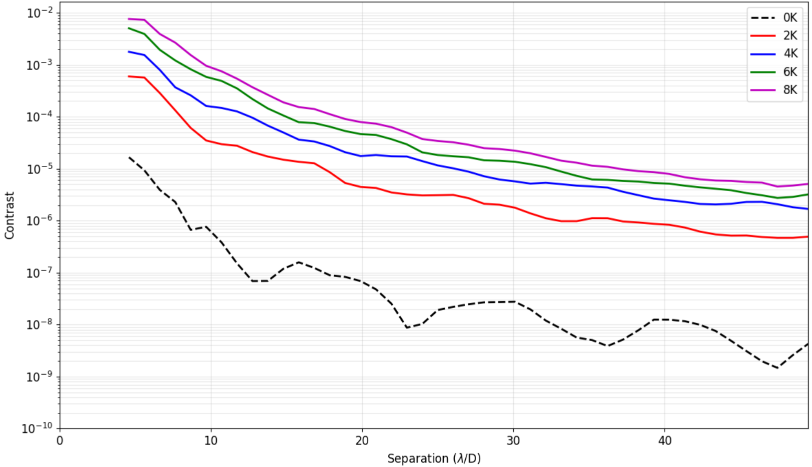

Contrast curves from simulated coronagraphic images for different spyder temperature

Table of Contents

- The **Low Wind Effect (LWE)** was successfully reproduced using the preliminary model.
- All components of the workflow are operational: **Large Model, Vent Model, Main Model, and Optical Model**.
- The simulated OPD values are of the same order as observations, and the resulting Point Spread Functions show similar features.
- **Future work:**
  - Improve geometrical representation of the dome, telescope
  - Validate the model against observational data - wind and temperature measurement is necessary (temperature sensor on spider)
  - Test and evaluate mitigation strategies

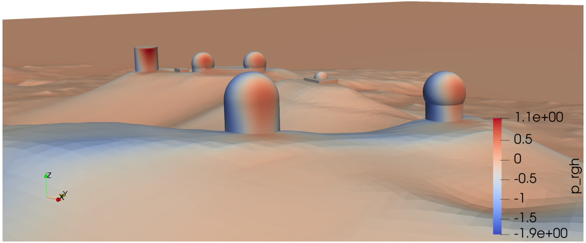

Static kinematic pressure distribution at the top of the Maunakea

The technical support and advanced computing resources from University of Hawaii Information Technology Services – Cyberinfrastructure, funded in part by the National Science Foundation CC* awards # 2201428 and # 2232862 are gratefully acknowledged.